

## Viscoelastic modes in chiral liquid crystals

K A SURESH

Raman Research Institute, C.V. Raman Avenue, Bangalore 560 080, India

Email: suresh@rri.res.in

**Abstract.** Viscoelastic properties of liquid crystals are very important for applications like display technology. However, there are not many direct techniques to study them. In this review, we describe our studies on the viscoelastic modes of some chiral liquid crystals using dynamic light scattering. We discuss viscoelastic modes corresponding to the C director fluctuations in the chiral smectic C phase and the behaviour of the Goldstone-mode near the chiral smectic C–smectic A phase transition. In cholesteric liquid crystals, we consider the director fluctuations in a wavevector range comparable to the inverse pitch of the cholesteric. Here, the study of the scattered light in the vicinity of the Bragg reflection using a novel geometry will be presented.

**Keywords.** Liquid crystals; viscoelastic modes.

**PACS Nos** 61.30.-v; 42.25.Fx

### 1. Introduction

Liquid crystals or mesophases are states of matter with a molecular order between that of liquids and crystals. Liquid crystals exhibit interesting viscoelastic properties [1,2]. The study of viscoelastic modes in them is important not only in understanding the structural dynamics but also in selecting suitable materials for display devices. In liquid crystals, thermal fluctuations in the average direction of orientation of the molecules (the director) result in strong fluctuations in the dielectric tensor causing intense scattering of light. Dynamic light scattering (DLS) is a useful technique to study the fluctuations in the scattered intensity which in turn can reveal the dynamics occurring in the scattering medium [3]. In liquid crystals, DLS studies yield relaxation times of the modes of the director's thermal fluctuations. In this review, we describe our studies on the viscoelastic modes in some chiral smectic C liquid crystals and in cholesteric liquid crystals.

Chiral smectic C liquid crystal ( $Sc^*$ ) has a helical structure of layers having uniformly tilted molecules. The director makes a constant angle with the layer normal and rotates uniformly from one layer to another. The tilt  $\theta$  and the azimuth  $\phi$  of the director are the amplitude and phase of the order parameters in the  $Sc^*$  phase respectively. The temperature fluctuations of the director leads to fluctuation in the tilt and azimuth giving rise to strong scattering of light. DLS is a useful technique to study the fluctuations at the  $Sc^*$ –Smectic A transition ( $T_c$ ) and in the  $Sc^*$  phase [4,5]. The soft mode is associated with the fluctuations in the tilt angle and the Goldstone-mode is associated with the fluctuations in the azimuth [4,6]. In the vicinity of the direct beam for a sample aligned in the Bragg mode and

in the vicinity of any diffraction order in the phase grating mode, the fluctuations in the intensity will reveal these modes. We have reported the measurement of relaxation time of the Goldstone-mode to determine the ratio of viscosity coefficient to elastic constant [7]. The determination of such a parameter is very useful in the application of chiral smectic C liquid crystals to optical devices like light modulators and display devices [8,9].

In a cholesteric liquid crystal (cholesteric), the director twists uniformly about a particular direction giving rise to a helicoidal structure of a definite pitch. Theoretical studies predict [1,10,11] the existence of two distinct modes of director fluctuations with wavevectors parallel to the helix axis. These are (i) the twist mode, with director fluctuations perpendicular to the helix axis and (ii) the umbrella mode, with out-of-plane director fluctuations [1]. Both these modes couple strongly to light. In spite of their importance in the understanding of the structural dynamics of cholesterics, in literature, there have been very few experimental investigations on these modes. Duke and Du Pre [12,13] studied these modes in a lyotropic cholesteric whose wavevector was about two orders of magnitude smaller than the wavevector of light. Their studies were carried out in the frequency domain in which they observed the broadening of the Rayleigh lines corresponding to the two modes. The large difference between the wavelength of light and the cholesteric pitch did not allow them to probe the dynamics of the cholesteric structure on length scales comparable to the pitch. Borsali *et al* [14] have measured the twist viscoelastic coefficient,  $k_{22}/\gamma_1$ , at room temperature for a cholesteric with and without a polymer additive. These systems were also probed with light whose wavevector is about 20 times larger than that of the cholesteric system.

We have reported a study of the twist mode which yields the viscoelastic coefficient  $k_{22}/\gamma_1$  [15]. The novelty in this study was the application of the Bragg reflection, a phenomenon arising out of the optical periodicity of the cholesteric, to locate the scattering wavevector at which one gets a minimum in the dispersion curve. The dispersion relation gives the dependence of the inverse relaxation time on the wavevector. Here, the scattering wavevector  $\mathbf{q}$  can be made parallel to the cholesteric twist axis. This enables one to select the modes with wavevectors parallel to the twist axis. Further, in the experiment the light scattered can be determined in the vicinity of the Bragg reflection, where the twist mode's contribution is very dominant [1,10]. The twist mode fluctuations involve winding and unwinding of the helical cholesteric structure. We describe the study of the twist mode as a function of temperature in a wavevector regime comparable to the equilibrium wavevector of the cholesteric.

## 2. Theory

### *Chiral smectic C*

In the case of chiral smectic C phase, one can write the relaxation time of the Goldstone-mode [4,5] as

$$\frac{1}{\tau_G} = \frac{K_2}{\gamma} (q_z - q_0)^2 + \frac{K_+}{\gamma} q_x^2, \quad (1)$$

where  $q_0$  is the wavevector of the helix and is given by the relation  $q_0 = 2\pi/P$ ,  $P$  being the pitch of the helix.  $q_x$  and  $q_z$  are the scattering wavevector components along  $x$ - and

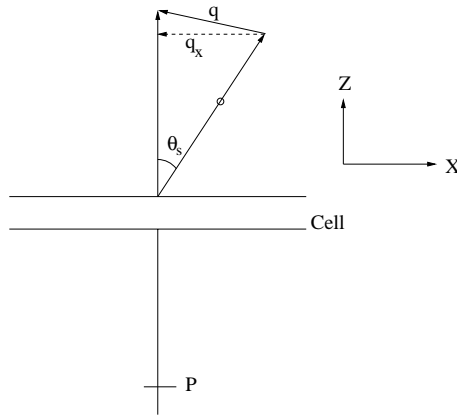


**Figure 1.** The scattering geometry used for a homeotropically aligned sample.

$z$ -direction respectively,  $\gamma$  is the viscosity coefficient. Here the twist axis is taken along the  $z$ -axis in the laboratory frame.  $K_+$  is given by  $K_+ = (K_1 + K_3)/2$ .  $K_1$ ,  $K_2$  and  $K_3$  are analogous to the usual splay, twist and bend elastic constants respectively.

In the homeotropic geometry, for small scattering angles  $\theta_s$  (see figure 1), we can write

$$q_z = q \sin(\theta_s/2) \quad \text{and} \quad q_x = q \cos(\theta_s/2), \quad (2)$$

where  $q = 2k_i \sin(\theta_s/2)$ ,  $k_i = 2\pi/\lambda$ . Here  $q$  is the magnitude of the scattering wavevector  $\mathbf{q}$ ,  $k_i$  the magnitude of the incident wavevector  $\mathbf{k}_i$  and  $\lambda$  the wavelength of light. At a given temperature the relaxation time data at different scattering angles were fitted to eq. (1) and the ratios of  $K_+/\gamma$  and  $K_2/\gamma$  were extracted.

### Cholesteric liquid crystal

In cholesterics, the director fluctuations are treated as thermally induced perturbations about the equilibrium structure [1]. The director is represented by a vector  $\mathbf{n}$ . Assuming the twist axis to be along the  $z$ -direction, the director components in the presence of only twist fluctuations can be described by

$$n_x = \cos(q_0 z + u), \quad (3)$$

$$n_y = \sin(q_0 z + u), \quad (4)$$

$$n_z = 0, \quad (5)$$

where  $u \equiv u(z, t)$  is a dimensionless fluctuation amplitude and  $q_0 = 2\pi/P$ , with  $P$  being the pitch of the helix. The amplitude of the fluctuation  $u$  can be decomposed into its Fourier components:

$$u(z, t) = \sum_{l=-\infty}^{\infty} u_l(t) e^{ilz}, \quad (6)$$

where  $u_l(t)$  is the amplitude of the  $l$ th component of wavevector  $l$ . The twist deformation leads to the off-diagonal element  $\epsilon_{xy}$  of the dielectric tensor [1]. This is given by

$$\epsilon_{xy} = \epsilon_a \{n_x \delta n_y + n_y \delta n_x\} \quad (7)$$

$$= \frac{\epsilon_a}{2} \sum_l \{e^{i2q_0 z} + e^{-i2q_0 z}\} u_l(t) e^{ilz}. \quad (8)$$

Here,  $\epsilon_a$  is the dielectric anisotropy of the medium and  $\delta n_x$  and  $\delta n_y$  are the fluctuations in the director components  $n_x$  and  $n_y$  respectively.

Thus, in general,  $\epsilon_{xy}$  is associated with the scattering wavevector

$$q = l \pm 2q_0. \quad (9)$$

For pure twist deformations in cholesterics, we can write the distortion-free energy density [1] as

$$F_d = \frac{k_{22}}{2} (\mathbf{n} \cdot (\nabla \times \mathbf{n}) + q_0)^2 \quad (10)$$

$$= \frac{k_{22}}{2} \left( \frac{\partial \theta'}{\partial z} - q_0 \right)^2. \quad (11)$$

Here,  $\theta' = (q_0 z + u(z, t))$  and  $k_{22}$  is the twist elastic constant.

The Langevin equation for the dynamical variable  $\theta'$  is

$$\gamma_1 \frac{\partial \theta'}{\partial t} = - \frac{\delta F_d}{\delta \theta'}, \quad (12)$$

where the right-hand side is the functional derivative of  $F_d$  and  $\gamma_1$  is the twist viscosity coefficient. Now,

$$\frac{\delta F_d}{\delta \theta'} = -k_{22} \frac{\partial^2 \theta'}{\partial z^2}. \quad (13)$$

Hence we get

$$\gamma_1 \frac{\partial \theta'}{\partial t} = k_{22} \frac{\partial^2 \theta'}{\partial z^2} \quad (14)$$

which leads to

$$\gamma_1 \frac{\partial u(z, t)}{\partial t} = k_{22} \frac{\partial^2 u(z, t)}{\partial z^2}. \quad (15)$$

In the Fourier space, the equation of motion for the  $l$ th Fourier component is

$$\gamma_1 \frac{\partial u_l(t)}{\partial t} = -k_{22} l^2 u_l(t). \quad (16)$$

Hence, we can obtain an expression for the relaxation time  $\tau_l$  of the amplitude of the fluctuation with wavevector  $l$ ,

$$\frac{1}{\tau_l} = \frac{k_{22}l^2}{\gamma_1}. \quad (17)$$

In a cholesteric,  $2q_0$  is the wavevector corresponding to the optical periodicity sensed by the incident light. Thus, it can be seen from eq. (17) that the relaxation time of the twist fluctuation goes to infinity as  $l \rightarrow 0$  or equivalently, as  $q \rightarrow \pm 2q_0$ . This result can be understood intuitively by looking upon the equilibrium twist of the cholesteric as a 'frozen in' fluctuation having an infinitely long relaxation time.

The director fluctuations couple to the incident light via the dielectric tensor. Fluctuations of the dielectric tensor gives rise to the scattering of incident light. The intensity of the scattered light can be studied for its autocorrelation. The intensity autocorrelation function is related to the electric field autocorrelation function via the Siegert relation [16]

$$g_2(\tau, q) = 1 + \beta |g_1(\tau, q)|^2. \quad (18)$$

Here,  $g_2(\tau, q)$  and  $g_1(\tau, q)$  are respectively the intensity and the electric field autocorrelation functions. The parameter  $\beta$  is a coherence factor that depends on experimental conditions like coherence area, average intensity and so on. It is a measure of the signal-to-noise ratio in the experiment. The autocorrelation is with respect to  $\tau$ , the delay time. The relaxation time of the dynamics occurring on the length scale  $q^{-1}$  is obtained by analysing the decay of  $g_2(\tau, q)$ .

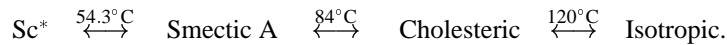
### 3. Experimental

#### *Chiral smectic C*

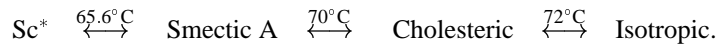
In this, experiments were carried out both in the homeotropic (smectic layers parallel to the glass substrate) and homogeneous (smectic layers perpendicular to the glass substrate) geometries. For the homeotropic alignment, the cleaned glass plates were coated with ODSE (0.1% octadecyl triethoxy silane in toluene solvent) and cured at 150°C. For the homogeneous alignment the glass plates were coated with the polyimide solution and cured at 300°C. Then the glass plates were rubbed in the preferred direction.

The materials used were SCE6, ZL5014-100 and SCE13 and their transition temperatures were as follows:

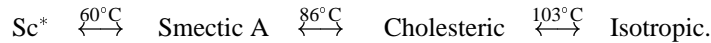
SCE6:



ZL5014-100:



SCE13:



Light from a He-Ne 35 mw laser ( $\lambda = 0.6328 \mu\text{m}$ ) with polarization parallel to the scattering plane was incident normally on the sample. The scattered light was analysed perpendicular to the scattering plane. A photon correlator (Malvern 4700c) was used to

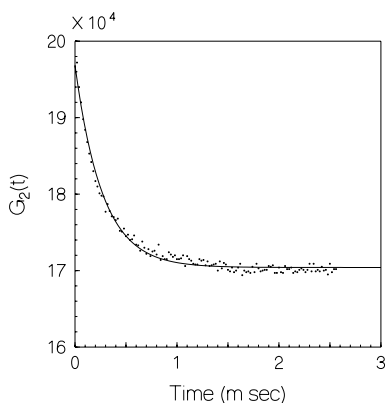


**Figure 2.** The intensity autocorrelation data obtained for SCE6 at 2.0°C below smectic A–Sc\* transition temperature ( $T_c$ ). The data is fitted to a single exponential.

acquire the intensity autocorrelation data. A typical intensity autocorrelation data obtained for SCE6 is shown in figure 2. This intensity autocorrelation was fitted to an exponential function given by

$$G(t) = a + b \exp(-t/\tau), \quad (19)$$

where  $\tau$  is the relaxation time,  $a$  represents the baseline and  $b$  depends on the experimental conditions. Experiments were performed at various scattering angles for fixed temperatures.

The appearance of the diffraction pattern as one cools the sample from the smectic A phase also indicates the phase transition to the Sc\* phase. The pitch of the materials in the Sc\* phase was obtained by measuring the angle of diffraction of the first order in the phase grating mode [17,18].

### *Cholesteric liquid crystal*

Here, mixtures of cholesterics with opposite helicities in various proportions were prepared to get a cholesteric of a pitch comparable to the wavelength of light. The sample used in the experiment was a three-component mixture of cholesteryl chloride, cholesteryl nonanoate and cholesteryl oleyl carbonate. These were taken in the proportions 63.8%, 26.5% and 9.7% respectively which yielded a right-handed cholesteric with a cholesteric-to-isotropic transition temperature of 62.8°C. The sample was filled into a cell and treated to get a planar alignment in the cholesteric phase. The cell was placed in a specially designed oven. The oven had a cylindrical cross-section, and was filled with glycerin which acted both as an index matching fluid and heat transferring medium. A cross-sectional side view of the sample cell placed in the oven is shown in figure 3. The light scattered by the sample in the cell was detected by a photomultiplier tube. For a certain orientation of the cell with respect to the incident light, the prominent Bragg reflection could be seen in the back scattering geometry. The scattered intensity was analysed in the vicinity of the Bragg reflection since the amplitude of the twist fluctuation is very large in this angular range.

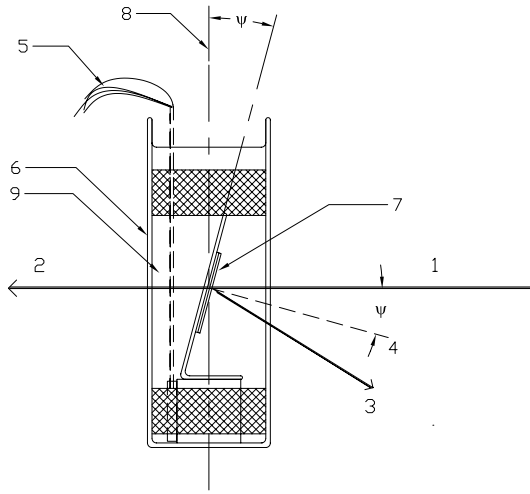


**Figure 3.** A cross-sectional side view of the sample cell placed inside the refractive index matched oven. (1) Incident beam, (2) unscattered beam, (3) the specular reflection from the front of the sample cell, (4) cell normal, (5) electrical leads for the heaters and resistance temperature device, (6) cylindrical glass tube, (7) sample cell containing the cholesteric liquid crystal, (8) goniometer and oven axis and (9) refractive index matching and heat transfer medium. The angle  $\psi$  is in a plane perpendicular to the scattering plane and it is highly exaggerated in the figure. In the experiment, it is less than  $2^\circ$  degrees through which the sample cell is tilted downwards, away from the scattering plane. Since the detector is sufficiently far away from the sample, this small angle tilt is enough to prevent the specularly reflected beam from entering the detector.

Using eqs (6)–(11) and applying the equipartition theorem, the expression for the thermal square amplitude of  $u_l$  can be obtained as

$$\langle |u_l|^2 \rangle = \frac{k_B T}{k_{22} l^2}. \quad (20)$$

Here,  $k_B$  is the Boltzmann constant and  $T$  the absolute temperature. It can be seen that as  $q \rightarrow \pm 2q_0$ ,  $l \rightarrow 0$  and the factor  $\langle |u_l|^2 \rangle$  diverges.

In the experiment, the intense static Bragg scattered beam was prevented from entering the detector. Thus the mode of light detection will be homodyne. Further, an analyser was used to minimize stray light entering the detector. The minimum in the twist dispersion curve occurs when the Bragg condition is satisfied. A schematic representation of the scattering geometry is shown in figure 4.

The pitch of the sample was determined from its transmission spectrum using a double beam spectrophotometer (Hitachi U-3200). The well-defined minimum,  $\lambda_0$ , at the center of the Bragg reflection band in the spectrum is related to the pitch [1] of the cholesteric by

$$\lambda_0 = \bar{\mu} P.$$

Here,  $\bar{\mu}$  is the average refractive index of the medium. The temperature dependence of  $P$  obtained using this method is shown in figure 5.

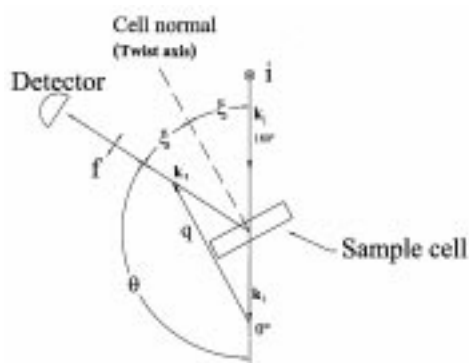


**Figure 4.** The scattering geometry used in the experiment. Here, the sample is aligned such that the twist axis is parallel to the cell normal. The vectors  $\mathbf{k}_i$ ,  $\mathbf{k}_f$  and  $\mathbf{q}$  are the incident, final and the scattering wavevectors respectively, while the vector  $\mathbf{i}$  is the polarisation direction of the incident light and  $\mathbf{f}$  is the polarisation direction in which the scattered light is analysed. The angle made by the cell normal (twist axis) with respect to the incident light is  $\xi$  and can be adjusted each time such that  $\mathbf{q}$  is parallel to the twist axis. The angle  $\xi$  is in the scattering plane. The magnitude of the wavevector  $\mathbf{q}$  is given by  $q = (4\pi\bar{\mu}/\lambda)\sin(\theta_s/2)$ , where  $\theta_s$  is the scattering angle;  $\lambda = 488$  nm, is the wavelength of light and  $\bar{\mu} = 1.5$  is the average refractive index of the scattering medium.

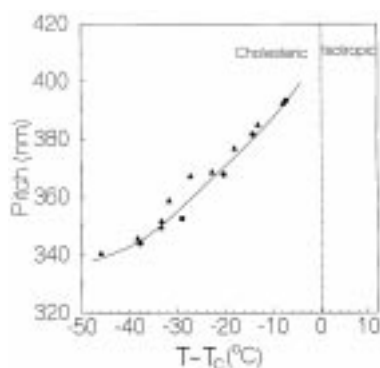


**Figure 5.** Variation of the pitch with temperature obtained by (●) selective reflection experiments, (▲) fitting the dispersion curves from the DLS experiments. The cholesteric-isotropic transition temperature,  $T_c$  is 62.8°C. The solid line is a cue to the eye.

Light from a 488 nm argon ion laser (Spectra Physics, model 163c), polarized perpendicular to the scattering plane was incident on the sample cell kept inside the oven at the center of the goniometer. The scattered light was detected by a photon counting photomultiplier tube (Electron Tubes Ltd., 9863/KB) whose output was fed to an amplifier-discriminator followed by a digital correlator (Malvern 4700c).

In the experiments, the following method was adopted to ensure that the scattering wavevector was parallel to the twist axis for every scattering angle. Laser light,

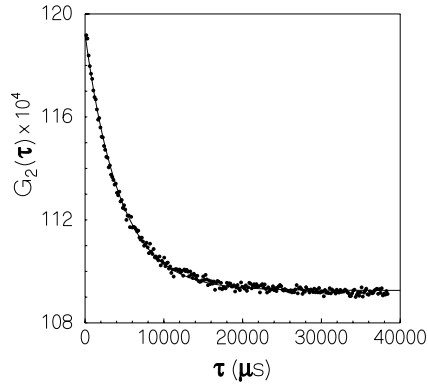


**Figure 6.** A typical un-normalized intensity correlogram obtained in the experiment. The data was taken at a scattering angle ( $\theta_s$ ) of  $95^\circ$  and with a delay time of  $150 \mu\text{s}$ . The total integration time was 300 s. The solid line is a theoretical fit with single exponential decay.

polarized vertically with respect to the scattering plane, was made to fall on the sample cell positioned at the center of the goniometer. The cell was then rotated about an axis perpendicular to the scattering plane until a prominent, but slightly broad Bragg reflection could be observed on a white screen placed in front of the cell. At the center of the Bragg spot, a faint but sharp specular reflection could be observed. This was the specular reflection of the incident beam from the sample cell surface. The cell was now rotated slightly away from the Bragg angle. Here, the Bragg spot became very weak and only the specular reflection remained on the screen. The detector was positioned along the direction of the specular reflection. Then, the specular reflection was prevented from entering the detector by very slightly tilting the cell normal downwards, through an angle  $\psi$ , away from the scattering plane. This arrangement is shown in figure 3. In this position, the projection of the cell normal in the scattering plane exactly bisects the angle made by the incident wavevector,  $\mathbf{k}_i$ , and the scattered wavevector,  $\mathbf{k}_f$ , as shown in figure 4. Then the scattering wavevector  $\mathbf{q}$  will be parallel to the cell normal, which is, in principle, the direction of the twist axis. This procedure of simultaneously reorienting the sample cell and the detector such that the cell normal exactly bisected the angle  $2\xi$  between  $\mathbf{k}_i$  and  $\mathbf{k}_f$ , was carried out for every scattering angle. Thus, it was ensured that for every angle,  $\mathbf{q}$  was parallel to the cell normal (twist axis).

In figure 6 we show a typical correlogram obtained in the experiments. Such an un-normalized correlogram is denoted by  $G_2(\tau)$ . Curve fitting is performed after normalizing such data with respect to their baselines. The baseline is automatically calculated by the correlator using very long sample times and it yields the value  $G_2(\infty)$ . The normalized correlogram  $g_2(\tau, q)$  is given by  $G_2(\tau)/G_2(\infty) - 1$ . Assuming that in the scattering geometry, the detected intensity fluctuations are predominantly due to the twist mode, one can fit the following function to the normalized data:

$$g_2(\tau, q) = a_1 + \beta e^{-2(\tau/\tau_r(q))}. \quad (21)$$

Here,  $a_1$  is the baseline and  $\tau_r(q)$  the relaxation time of the fluctuations of wavevector  $q$ . For the twist mode fluctuations

$$\tau_r(q) = \tau_{q \pm 2q_0}. \quad (22)$$

The values of the parameters  $a_1$ ,  $\beta$  and  $\tau_r(q)$  are obtained from standard non-linear curve fitting routines. The twist dispersion curve at a given temperature is obtained by plotting the inverse of the relaxation time as a function of  $q$ . By fitting such a curve to a generalized second degree function of  $q$ , both  $q_0$  and  $k_{22}/\gamma_1$  can be obtained.

In birefringent systems, the magnitudes of the scattered wavevector will generally differ from the magnitude of the incident wavevector. When the birefringence is small, the magnitude of the scattered and incident wavevectors can be considered to be equal, that is, the scattering is quasi elastic. A cholesteric can be looked upon as an uniform helical stack of birefringent layers. If the birefringence  $\Delta\mu$  of such a layer is small, the angular dependence in  $q$  is only through the  $\sin(\theta_s/2)$  factor. In the analysis, the average refractive index  $\bar{\mu}$  and the layer birefringence  $\Delta\mu$  have been taken equal to 1.5 and 0.05 respectively. These are close to the values reported in the literature.

#### 4. Results and discussion

Temperature dependence of the helical pitch of the three chiral smectic C materials are shown in figure 7. The pitch of SCE13 is almost constant in the Sc\* phase. The temperature dependence of the relaxation time across the smectic A–Sc\* transition for homogeneously aligned SCE6 is shown in figure 8. Here, the inverse of the relaxation time corresponding to the degenerate mode in the smectic A phase drops sharply at the smectic A–Sc\* transition. One may notice that the Goldstone-mode in the Sc\* phase has an almost constant relaxation time. Scattering angle dependence of the inverse of the relaxation time of the Goldstone-mode in the homeotropically aligned Sc\* phase for the SCE6 material is shown in figure 9. As expected from the simple elastic theory, the inverse of the relaxation time is dependent quadratically on the scattering angle. Similar dependence exists in all the three materials. Hence eq. (1) can be fitted with the data to extract the values of  $K_+/\gamma$  and  $K_2/\gamma$  at different temperatures. The calculated values of  $K_+/\gamma$  and  $K_2/\gamma$  for the three materials SCE6, ZL5014-100 and SCE13 are shown in tables 1, 2 and 3. These values do not follow a regular trend with temperature. However, the values are of the same order of magnitude as those reported in literature for chiral smectic C liquid crystals [5,19–21].

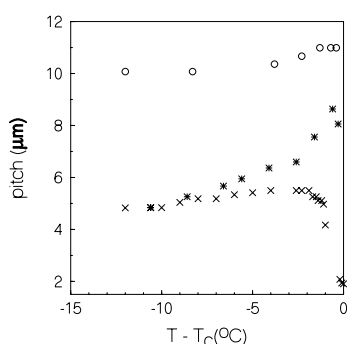


**Figure 7.** The measured pitch for the materials as a function of temperature. The symbols  $\times$ ,  $*$  and  $\circ$  represents the data for SCE6, ZL5014-100 and SCE13 respectively.

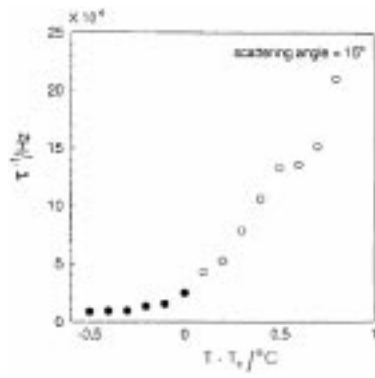


**Figure 8.** The inverse of the relaxation time  $\tau^{-1}$  across the smectic A-to-Sc\* phase transition for SCE6. The open circles represent the inverse of the relaxation time corresponding to the degenerate mode in the smectic A phase. The dark circles represents the Goldstone-mode in the Sc\* phase. The data was taken for a homogeneously aligned sample at a constant scattering angle.

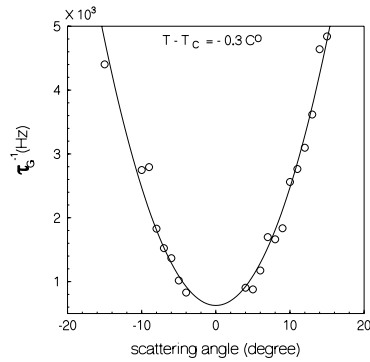


**Figure 9.**  $\tau_G^{-1}$  corresponding to the Goldstone-mode relaxation as a function of scattering angle for SCE6 in the Sc\* phase. The data is fitted to the quadratic function of scattering angle.

**Table 1.** Viscoelastic coefficients for the SCE6 at different temperatures.

$T - T_c$ ( $^\circ$ C)	$K_2/\gamma$ ( $\text{cm}^2 \text{s}^{-1}$ )	$K_+/\gamma$ ( $\text{cm}^2 \text{s}^{-1}$ )
-0.3	$1.08 \pm 0.135 \times 10^{-6}$	$2.82 \pm 0.350 \times 10^{-7}$
-1.3	$4.05 \pm 0.848 \times 10^{-6}$	$5.08 \pm 0.722 \times 10^{-7}$
-2.3	$6.36 \pm 0.529 \times 10^{-6}$	$7.33 \pm 0.609 \times 10^{-7}$
-3.3	$7.79 \pm 0.569 \times 10^{-6}$	$8.98 \pm 0.655 \times 10^{-7}$
-4.3	$8.43 \pm 0.960 \times 10^{-6}$	$9.72 \pm 0.110 \times 10^{-7}$
-5.0	$7.26 \pm 0.619 \times 10^{-6}$	$8.50 \pm 0.724 \times 10^{-7}$
-9.3	$7.24 \pm 0.693 \times 10^{-6}$	$9.16 \pm 0.876 \times 10^{-7}$

**Table 2.** Viscoelastic coefficients for the ZL5014-100 at different temperatures.

$T - T_c$ ( $^{\circ}\text{C}$ )	$K_2/\gamma$ ( $\text{cm}^2 \text{s}^{-1}$ )	$K_+/\gamma$ ( $\text{cm}^2 \text{s}^{-1}$ )
-1.0	$4.55 \pm 1.40 \times 10^{-6}$	$3.57 \pm 1.32 \times 10^{-7}$
-1.6	$9.91 \pm 1.94 \times 10^{-6}$	$8.35 \pm 1.63 \times 10^{-7}$
-2.6	$3.59 \pm 2.98 \times 10^{-6}$	$3.50 \pm 2.36 \times 10^{-7}$
-3.6	$5.62 \pm 1.13 \times 10^{-6}$	$5.63 \pm 1.12 \times 10^{-7}$
-4.6	$8.42 \pm 1.35 \times 10^{-6}$	$8.70 \pm 1.39 \times 10^{-7}$
-5.6	$5.19 \pm 1.60 \times 10^{-6}$	$5.59 \pm 1.70 \times 10^{-7}$
-10.6	$3.49 \pm 1.49 \times 10^{-6}$	$4.63 \pm 1.96 \times 10^{-7}$
-15.6	$3.37 \pm 1.51 \times 10^{-6}$	$4.76 \pm 1.11 \times 10^{-7}$

**Table 3.** Viscoelastic coefficients for the SCE13 at different temperatures.

$T - T_c$ ( $^{\circ}\text{C}$ )	$K_2/\gamma$ ( $\text{cm}^2 \text{s}^{-1}$ )	$K_+/\gamma$ ( $\text{cm}^2 \text{s}^{-1}$ )
-1.0	$2.22 \pm 0.663 \times 10^{-5}$	$1.27 \pm 0.363 \times 10^{-7}$
-2.0	$1.36 \pm 0.226 \times 10^{-5}$	$0.81 \pm 0.134 \times 10^{-7}$
-3.0	$1.95 \pm 0.255 \times 10^{-5}$	$1.18 \pm 0.154 \times 10^{-7}$
-4.0	$1.89 \pm 0.352 \times 10^{-5}$	$1.16 \pm 0.326 \times 10^{-7}$
-5.0	$1.34 \pm 0.386 \times 10^{-5}$	$0.83 \pm 0.239 \times 10^{-7}$
-8.7	$1.86 \pm 0.589 \times 10^{-5}$	$1.16 \pm 0.368 \times 10^{-7}$

An interesting result of this study is the observation of a new relatively slow relaxation mode in SCE6 material, in addition to the Goldstone-mode, in a sample aligned in the homogeneous geometry. The relaxation time of the slow mode was nearly independent of the scattering angle. It is worth noting that this slow relaxation mode is not observed in the homeotropically aligned sample and only present in the sample aligned in the homogeneous geometry. It is well-known that a chiral smectic C liquid crystal with high polarization placed under an external biased electric field or confined in a restricted geometry can give rise to additional modes which try to recover the broken helicoidal symmetry [22,23]. One can attribute the origin of the slow mode in SCE6, to the boundary effects which can deform the helical structure of the  $\text{Sc}^*$  phase. However, this type of slow mode was not observed in ZL5014-100 and SCE13 samples, even though the cell thicknesses used were comparable to that of SCE6. It is interesting to probe this mode as a function of sample thickness and in the presence of an external applied DC electric field.

In the case of cholesteric liquid crystals, dispersion curves for the twist fluctuations have been obtained in a wavevector range in the neighbourhood of the equilibrium cholesteric wavevector. A typical dispersion curve is depicted in figure 10. From the dispersion curves obtained at various temperatures we have evaluated the temperature dependence of the viscoelastic coefficient  $k_{22}/\gamma_1$ . It can be seen from eq. (17) that the twist mode relaxation frequency should be exactly zero at  $q = \pm 2q_0$ . But our results indicate the presence of a finite relaxation frequency at  $2q_0$ . The finite non-zero relaxation frequency at  $q = 2q_0$  in the dispersion curves, could be either due to contributions from the umbrella mode or from modes which might arise due to non-uniformities in the orientation of the helix axis.

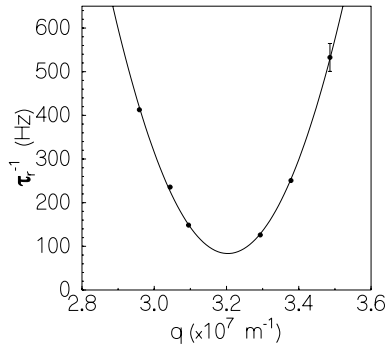


**Figure 10.** Dispersion curve of the twist mode obtained in a wavevector range in the neighbourhood of the equilibrium cholesteric wavevector at a temperature of  $50 \pm 0.05^\circ\text{C}$ . The solid line is a least square quadratic fit to the experimental points. The value of  $k_{22}/\gamma_1$  obtained from this data set is  $(5.588 \pm 0.007) \times 10^{-11} \text{ m}^2\text{s}^{-1}$ .

The assumption that the helix axis is exactly parallel to the cell normal over the entire scattering volume is not true in practice. In an actual sample, there always will be some non-uniformities in the cholesteric structure arising due to defects on the bounding surfaces leading to misalignments in the twist axis. Such misalignments in the twist axis can lead to a small contamination of the scattered light from the umbrella mode. Due to this, the autocorrelation function of the scattered intensity is not exactly described by a single exponential. This is revealed by a close examination of the tail of the correlogram. The small out-of-plane tilt,  $\psi$ , imparted to the sample may also result in a slight contribution from other modes. Such contributions from other modes may explain the gap in the twist mode dispersion curves. Drevěšek *et al* [24] and Muševič *et al* [25] also give a similar explanation to account for the gap found in the dispersion curves for chiral smectic C. We believe that the dominant contribution to the scattered intensity is due to the twist mode and have analysed the data accordingly.

The minimum in the dispersion curve occurs at a value of  $q$  which corresponds to  $2q_0$ . From the value of  $q_0$  thus obtained, one can evaluate the pitch of the cholesteric system. We find a good agreement between the values of the pitch obtained by fitting the dispersion curves and those obtained by the reflection spectroscopy experiments (figure 5). They reveal that the pitch of the cholesteric mixture increases with temperature. The increase in pitch causes the Bragg reflection angle to decrease.

For temperatures close to the cholesteric–isotropic transition, the Bragg reflected light was not accessible in the set up. But the trend in the temperature behaviour of the viscoelastic coefficient  $k_{22}/\gamma_1$  is clearly borne out by the data obtained from the experimentally accessible scattering wavevectors. The temperature variation of the twist viscoelastic coefficient is shown in figure 11.

Borsali *et al* [14] have studied the modes of director fluctuations in a cholesteric system where the pitch was  $10 \mu\text{m}$  ( $q_0 \approx 0.6 \times 10^6 \text{ m}^{-1}$ ). The wavelength of light used in their experiments was about 20 times smaller than the pitch of the cholesteric. In our experiments, the pitch of the cholesteric is of the order of  $0.4 \mu\text{m}$  ( $q_0 \approx 16 \times 10^6 \text{ m}^{-1}$ ) and the wavelength of light is  $0.488 \mu\text{m}$ . This combination of pitch and wavelength allows us to probe the fluctuations of the cholesteric structure on length scales comparable to the pitch.

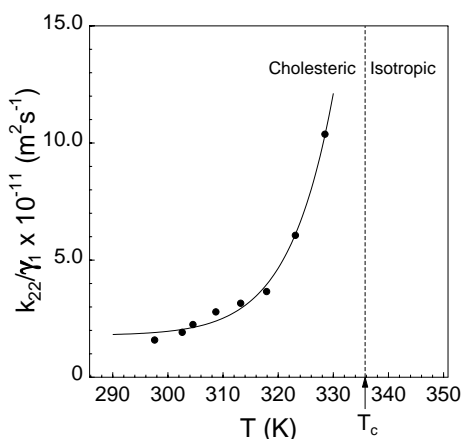


**Figure 11.** The twist viscoelastic coefficient  $k_{22}/\gamma_1$  as a function of temperature. The cholesteric–isotropic transition temperature,  $T_c$ , is 335.8 K. The solid line is a fit to an exponential function of the form  $b_1 + b_2 e^{-E_a/k_B T}$  to the data. Here,  $b_1$  and  $b_2$  are fit parameters. The value of  $E_a$  has been taken to be 1.16 eV.

Another advantage of having the cholesteric pitch comparable to the wavelength of light is that one can utilize the Bragg reflection to locate the range of wavevectors over which the twist mode is most dominant. We have experimentally obtained the variation in the value of  $k_{22}/\gamma_1$  as a function of temperature and we find that  $k_{22}/\gamma_1$  increases sharply as one approaches the cholesteric–isotropic transition temperature.

In the geometry used by Borsali *et al* the component of the scattering wavevector perpendicular to the twist axis ( $q_{\perp}$ ), is assumed to be much smaller than  $q$  and hence the component parallel to the twist axis ( $q_{\parallel}$ ) was considered to be nearly equal to  $q$ . In our geometry, by suitably adjusting the orientation of the sample cell with respect to the incident beam, one can maintain  $q_{\perp} \sim 0$  and  $q_{\parallel} \sim q$  at all scattering angles. Interestingly, we find that the values of  $k_{22}/\gamma_1$  are about an order of magnitude higher compared to the values in their cholesteric system [14]. This is very likely due to the fact that the cholesteric molecules in our system are bulkier than the molecules in their system. Also, they find that in the presence of a polymer additive, the value of  $k_{22}/\gamma_1$  reduces. Incidentally, the values of the twist viscoelastic coefficient for cholesterics are much lower than those in the chiral smectic phases [7]. In addition, the viscoelastic coefficients of the cholesteric system show a monotonic trend as a function of temperature unlike those in the chiral smectic phases.

There have been a few reports on the measurements of the twist viscoelastic coefficient  $k_{22}/\gamma_1$  for nematic liquid crystals in the literature [26–28]. Sefton *et al* [26] have carried out dynamic light scattering experiments to determine  $k_{22}/\gamma_1$  for pure nematic pentylcyanobiphenyl (5CB) and for the system doped with different amounts of a polymeric side chain liquid crystal. Their values of the twist viscoelastic coefficient  $k_{22}/\gamma_1$  are comparable to those obtained by us. As a function of increasing temperature, they observe a non-linear increase in the value of  $k_{22}/\gamma_1$ . Gu *et al* [27] and recently Borsali *et al* [28] have also reported measurements of  $k_{22}/\gamma_1$  of the same nematic liquid crystal, 5CB. Though our system is cholesteric, the values of  $k_{22}/\gamma_1$  are of the same order of magnitude reported in nematics [26–28].

Assuming the usual temperature dependence of  $\gamma_1$  and  $k_{22}$  of nematics [29], we have compared our results on the variation of  $k_{22}/\gamma_1$  as a function of temperature. We take the temperature dependence of the viscosity coefficient  $\gamma_1$  to be

$$\gamma_1(T) \propto S(T)e^{(E_a/k_B T)}, \quad (23)$$

where  $S$  is the orientational order parameter and  $E_a$  the activation energy. We take the temperature dependence of  $k_{22}$  to be

$$k_{22}(T) \propto S^2(T). \quad (24)$$

For comparison, we fit our data to a function of the form

$$b_1 + b_2 S(T)e^{(-E_a/k_B T)}, \quad (25)$$

where  $b_1$  and  $b_2$  are fit parameters, and  $E_a$  is taken to be 1.16 eV. The  $S(T)$  values for a nematic are taken from the literature [2]. Over the temperature range in which the experiment was performed, the magnitude of  $S(T)$  remains almost constant and can be absorbed in the parameter  $b_2$ . The fit is shown as a solid line in figure 11. It shows a reasonably good agreement.

We have studied the temperature dependence of the pure twist viscoelastic mode in a thermotropic cholesteric. We have selected a combination of pitch and the wavelength of light that allows us to investigate twist fluctuations of cholesterics on a length scale comparable to the pitch. Such studies give the values of twist viscoelastic coefficients which are very important to characterize cholesterics for device applications [30,31].

## References

- [1] P G De Gennes and J Prost, *The physics of liquid crystals*, 2nd edn. (Oxford University Press, Oxford, 1993)
- [2] S Chandrasekhar, *Liquid crystals*, 2nd edn. (Cambridge University Press, Cambridge, 1992)
- [3] B J Berne and R Pecora, *Dynamic light scattering* (John Wiley and Sons, New York, 1976)
- [4] I Muševič, R Blinc, B Žekš, C Filipič, M Čopič, A Seppen Wyder and A Levanyuk, *Phys. Rev. Lett.* **60**, 1530 (1988)
- [5] I Dervenšek, I Muševič and M Čopič, *Phys. Rev.* **A41**, 923 (1990)
- [6] T Carlsson, B Žekš, C Filipič, A Levstik and R Blinc, *Mol. Cryst. Liq. Cryst.* **163**, 11 (1988)
- [7] Yuvaraj Sah and K A Suresh, *Liq. Cryst.* **24**, 701 (1998)
- [8] M O Freeman, T A Brown and D M Walba, *Appl. Opt.* **31**, 3917 (1992)
- [9] N A Clark and S T Lagerwall, *Appl. Phys. Lett.* **36**, 899 (1980)
- [10] C Fan, L Kramer and M J Stephen, *Phys. Rev.* **A2**, 2482 (1970)
- [11] M S Veshchunov, *Sov. Phys. JETP* **49**, 769 (1979)
- [12] R W Duke and D B Du Pre, *Phys. Rev. Lett.* **33**, 67 (1974)
- [13] R W Duke and D B Du Pre, *Mol. Cryst. Liq. Cryst.* **43**, 33 (1977)
- [14] R Borsali, U W Schroeder, D Y Yoon and R Pecora, *Phys. Rev.* **E58**, R2717 (1998)
- [15] M S Giridhar and K A Suresh, *Euro. Phys. J.* **E7**, 167 (2002)
- [16] P A Lemieux and D J Durian, *J. Opt. Soc. Am.* **16**, 1651 (1999)
- [17] K A Suresh, Yuvaraj Sah, P B Sunil Kumar and G S Ranganath, *Phys. Rev. Lett.* **72**, 2863 (1994)
- [18] K Kondo, H Tekezoe, A Fukuda and E Kuze, *Jpn. J. Appl. Phys.* **21**, 224 (1982)

- [19] M H Lu, A Crandall and C Rosenblatt, *Phys. Rev. Lett.* **68**, 3575 (1993)
- [20] C Y Young, R Pindak, N A Clark and R B Meyer, *Phys. Rev. Lett.* **40**, 773 (1978)
- [21] D H Van Winkle and N A Clark, *Phys. Rev.* **A38**, 1573 (1988)
- [22] B Žekš, T Carlsson, I Mušević and Kutnjak-Urbanc, *Liq. Cryst.* **15**, 103 (1993)
- [23] Y P Panarin, H Xu, S T Mac Lughadha and J K Vij, *Jpn. J. Appl. Phys.* **33**, 2648 (1994)
- [24] I Drevenšek, I Mušević and M Čopič, *Phys. Rev.* **A41**, 923 (1990)
- [25] I Mušević, A Rastegar, M Čepič, B Žekš and M Čopič, *Phys. Rev. Lett.* **77**, 1769 (1996)
- [26] M S Sefton, A R Bowdler and H Coles, *Mol. Cryst. Liq. Cryst.* **129**, 1 (1985)
- [27] D Gu, A M Jamieson, C Rosenblatt, D Tomazos, M Lee and V Perc, *Macromolecules* **24**, 2385 (1991)
- [28] R Borsali, D Y Yoon and R Pecora, *J. Phys. Chem.* **B102**, 6337 (1998)
- [29] W H de Jeu, *Physical properties of liquid crystalline materials* (Gordon and Breach, London, 1980)
- [30] Masahito Oh-e and Katsumi Kondo, *Appl. Phys. Lett.* **69**, 623 (1996)
- [31] G P Gordon, *IEEE Spectrum*, October 2000